RSC Advances

PAPER

View Article Online
View Journal | View Issue

Cite this: *RSC Adv.*, 2016, **6**, 72230

Activation energies and information entropies of helium penetration through fullerene walls. Insights into the formation of endofullerenes *n*X@$C_{60/70}$ (n = 1 and 2) from the information entropy approach†

Denis Sh. Sabirov,*[a] Anton O. Terentyev[a] and Viacheslav I. Sokolov[b]

Received 11th May 2016
Accepted 25th June 2016

DOI: 10.1039/c6ra12228k

www.rsc.org/advances

In the present study, we calculate the activation barriers and information entropies of helium penetration into the C_{60} and C_{70} fullerenes resulting in the singly and doubly filled endofullerenes $He_n@C_{60/70}$ (n = 1 and 2). The activation barriers of hexagon penetration of C_{60} and C_{70} are very high (~900 kJ mol^{-1}) and they slightly increase for the second insertion as compared to the first step. The activation parameters are linearly correlated with the squares of the penetrated hexagons. This allows the proposal that the other fullerene cages should reveal almost the same penetrability because the size of the hexagons do not significantly vary from one fullerene to another. We have found that the experimental ratios of the yields of $He@C_{60/70}$ and $He_2@C_{60/70}$ (and the other related endofullerenes $Ne_n@C_{70}$, $(H_2)_n@C_{70}$, and $NHe@C_{60/70}$) may be qualitatively described in terms of the information entropy approach using the respective changes in information entropy upon the formation of singly and doubly filled endofullerenes. This approach stresses the probabilistic nature of the penetration processes and may be used for qualitative prediction of the expected yields of endofullerenes with two encapsulated species.

1 Introduction

Fullerenes due to their hollow structure are able to form endohedral complexes (endofullerenes), which are unique compounds encapsulating diverse atoms, molecules or clusters.[1–6] Among them, noble gas endofullerenes X@C_{60} (X = He–Xe) are the most studied because these species have been obtained and identified in the earliest studies on the fullerene chemistry (see the exhaustive introduction of study[7] and some key original studies[8–13]). Although some endohedral complexes of fullerenes have been proposed and tested as qubits of quantum computers (*e.g.*, N@C_{60})[14–16] and radiopharmaceuticals (Ac@C_{82}),[17] the interest in noble gas endofullerenes is currently fundamental rather than applied. Indeed, the encapsulation of noble gases allows monitoring of the interactions between guest and host molecules with minimal accompanying and interfering effects such as significant cage deformations or charge transfer.

The physical properties of X@C_{60} (X = He–Xe) have been studied both experimentally and theoretically. For example, the theoretical studies cover the aspects of their stability,[18–20] exohedral reactivity,[7,21] mechanical properties,[22] dipole polarizability,[23–25] and photoionization.[26] Mechanistic studies on the formation of the endofullerenes with noble gas atoms inside are scarce.[12,27–29] The relatively low activation barrier of the helium release by He@C_{60} (~3.5 eV) was the reason to consider that guest atoms should come into the fullerene interiors through the one-bond windows resulting from C–C bond cleavage. The activation barrier of the last process equals 3.5 eV according to the MNDO calculations of the triplet biradical C_{60} with one broken 5.6 bond (the bond common for pentagon and hexagon),[27] and this value is lower compared with the penetration through hexagon (~10.7 eV, estimated for the helium passage through the benzene ring[30] by MP2/6-31G** calculations). Furthermore, penetrations of helium through intact (*via* hexagon or pentagon) and damaged C_{60} cages (with one-bond and two-bond windows) have been thoroughly studied using the MNDO, HF/3-21G, BLYP/3-21G, and BP86/3-21G methods.[28] This computational study revealed very high (more than 800 kJ mol^{-1}) and close activation barriers for all the studied pathways, thus it was difficult to select the most preferable route of the process. The authors[28] considered that the activation barriers are decreased in the case of defected fullerene cages (with 4- and 8-membered cycles).

[a]*Institute of Petrochemistry and Catalysis, Russian Academy of Sciences, 450075 Ufa, Russia. E-mail: diozno@mail.ru; Fax: +7 347 284 27 50*

[b]*A. N. Nesmeyanov Institute of Organoelement Compounds, Russian Academy of Sciences, 119991 Moscow, Russia*

† Electronic supplementary information (ESI) available: Results of the B3LYP/Λ1 calculations; Cartesian coordinates of endofullerenes and transition states of their formation. See DOI: 10.1039/c6ra12228k

Although the mentioned studies were a breakthrough in understanding the formation of endohedral structures, these, however, operate with some assumptions such as the similarity of the input and output processes for moving an He atom through the fullerene cage and application of the one mechanistic model to different noble gases. It was also considered that C_{60} is reversibly damaged under the extreme conditions endofullerene synthesis (*e.g.*, 5 h, 600 °C, 2500 atm (ref. 12)). At the same time, it is known that this highly symmetric molecule is able to survive in much harsher conditions.[31] One of the explanations of the stability of fullerene-containing compounds deals with possible dissipation of the obtained redundant energy by the rich system of vibrational modes of the C_{60} framework.[32]

Thus, white spots remain in the mechanism of the fullerene cage penetration. We propose that some insights into this topic may come from a comparative study of helium penetration into the C_{60} and C_{70} fullerenes. Currently, the endohedral complexes of C_{60} and C_{70} with up to two trapped helium atoms are synthesized,[33,34] whereas the C_{60}-based endofullerenes have been widely investigated by theoretical methods, the endohedral complexes of C_{70}, the second abundant fullerene, are less studied. Previously, we studied the chemical transformations of $H_2O@C_{60}$,[35] $CH_4@C_{60}$,[36] and the C_{70} endohedral complexes with hydrocarbons[37] using DFT methods. In the present study, we use the proven computational methodology to study the formation of $He_n@C_{60}$ and $He_n@C_{70}$ ($n = 1$ and 2) focusing on intact C_{60} and C_{70} as starting structures.

2 Computational details

The scanning of potential energy surface (PES) and all optimizations were performed using the density functional theory method PBE/3ζ[38] implemented in the Priroda program.[39] The 3ζ basis set describes the electronic configurations of molecular systems by the orbital basis sets of contracted Gaussian-type functions (5s,1p)/[3s,1p] for He and (11s,6p,2d)/[6s,3p,2d] for C, which have been used in combination with the density-fitting basis sets of uncontracted Gaussian-type functions (5s,1p) for He and (10s,3p,3d,1f) for C atoms. The PBE/3ζ method reproduces structures and physicochemical characteristics of fullerenes and their derivatives with high accuracy (see reviews[40,41] and key works on its application in computational thermochemistry[42–47] and transition theory calculations of fullerene-containing systems[42,48–50]). Although the PBE/3ζ method was tested and efficiently used for endofullerene studies, we performed a recalculation of the key processes using the B3LYP/Λ1 method[51,52] to ensure the reliability of the obtained results (the Λ1 basis set includes the contracted Gaussian-type functions (6s,2p)/[2s,1p] for He and (10s,7p,3d)/[3s,2p,1d] for C combined with the uncontracted functions (6s,3p)/[2s,1p] for He and (10s,9p,7d,4f)/[6s,4p,3d,1f] for C atoms). This method was previously applied to the theoretical studies of fullerene derivatives. In all cases, the B3LYP/Λ1 results qualitatively mimic the regularities obtained by the main method, and these are presented in the ESI Materials.† The hessians of the minima of PESs (endofullerene molecules) contain no imaginary frequencies; the transition states (TSs) of their formation reveal one imaginary frequency with the main contribution corresponding to the motion of the helium atom through the fullerene wall. The correctness of the found TSs was confirmed by the intrinsic reaction coordinate calculations.

The heat effects of the insertion processes were calculated as the differences between the total energies E of the final endofullerene and its isolated components before the insertion, taking into account the zero-point vibrational energy corrections, ε_{ZPV}, and the temperature corrections, H_{corr} ($T = 298$ K):

$$\Delta H^\circ = (E_{tot} + \varepsilon_{ZPV} + H_{corr})_{endofullerene} - \sum_{He\ and\ fullerene} (E_{tot,i} + \varepsilon_{ZPV,i} + H_{corr,i}) \quad (1)$$

Analogously, the activation energies were calculated as the differences between the mentioned energetic parameters of the transition states of the processes and the initial endohedral complexes ($T = 298$ K):

$$E_{act} = (E_{tot} + \varepsilon_{ZPV} + H_{corr})_{TS} - \sum_{He\ and\ fullerene} (E_{tot,i} + \varepsilon_{ZPV,i} + H_{corr,i}) \quad (2)$$

Unfortunately, the Priroda program[39] does not implement facilities to take into account basis set superposition errors since they are usually included in similar calculations of endohedral complexes (see, *e.g.*, ref. 18–20). However, the error with respect to their neglect is substantially lower than the calculated activation energies (orders of magnitudes are $\sim 10^{0-1}$ *vs.* $\sim 10^2$ kJ mol^{-1}), thus the calculated values are suitable for qualitative mechanistic considerations. Such neglect was previously used in the studies of highly energetic physical[22,53] and chemical processes.[36,54]

To analyze the relation between the activation parameters and fullerene geometry, we calculated squares of the penetrated hexagons, which are auxiliary structural parameters. For this purpose, we divided the hexagons into four triangles, calculated their squares (substituting internuclear distances from the optimized geometries in Heron's equation), and summed them.

The application of the information theory approach[55–61] to endofullerenes was performed by distinguishing the inequivalent atoms in their structures, as in our previous studies.[62,63] Accordingly, the probability, p_i, of finding an atom of i type equals N_i/N where N_i is the number of i atoms and $N = \Sigma N_i$ is the total number of atoms in the molecule. Then, the information entropy (in bits) of the structure under consideration equals:

$$h = -\sum_i^n \frac{N_i}{\sum_i^n N_i} \log_2 \frac{N_i}{\sum_i^n N_i} \quad (3)$$

3 Results and discussion

3.1 Formation of He@C_{60} endofullerene

Previously, it has been shown that the helium atom is able to penetrate the fullerene cage through the window formed by the 5.6 C–C bond cleavage.[27,28] Moreover, according to calculations

by the semiempirical MNDO method, the structure with one broken 5.6 bond (in which the distance between the carbon atoms becomes 2.48 Å) corresponds to a local minimum of the triplet PES. We performed similar PES scanning *via* the DFT methods PBE/3ζ and B3LYP/Λ1 and found no local minima on the triplet PES: the total energy of the molecular system monotonously grows when the 5.6 bond is extended up to 5 Å (Fig. 1; the results of the B3LYP/Λ1 are presented in the ESI Materials†). Optimization of the triplet open-C_{60} structures with the bond elongated up to 2.694 and 3.857 Å led to restauration (we chose these distances because they have some "hints" to be the inflection points of the PES obtained by PBE/3ζ; note that there are no such "hints" in the case of the B3LYP/Λ1 scanning). This propensity for restauration of the initial structure was previously noted upon quantum chemical modelling of the compression of the endofullerenes $H_2O@C_{60}$ and $CH_4@C_{60}$.[35,36] The cited studies demonstrate that the C_{60} fullerene is able to restore its initial structure even from the deeper deformed (flattened) states, in which the topology of the carbon skeleton is broken and chemical bonds with fragments of the encapsulated molecules are formed.

As previously shown theoretically, helium may take two positions inside the C_{60} cage, resulting in two structures of $He@C_{60}$ with I_h (central position) and C_{2v} (off-center) symmetry point groups.[23] The calculated differences in the total energies and mean polarizabilities of $He@C_{60}$ with center and off-center positions are negligible.[23] X-ray experiments reveal that helium in $He@C_{60}$ is located at the center of the fullerene cage.[64] In our study, we focus on the of formation of the I_h-symmetrical $He@C_{60}$:

$$He + C_{60} \rightarrow He@C_{60} \quad (4)$$

This process is slightly endothermic: the calculated heat effect equals +5.3 kJ mol^{-1} (PBE/3ζ). The scanning of two possible helium penetrations (*via* hexagon or pentagon) into the fullerene cage without breaking chemical bonds was performed (Fig. 2). The structures, corresponding to the maxima of the singlet PESs, were used to search for the transition states (Table 1, Fig. 3). The hessian of the transition state of the penetration *via* the hexagon (TS_{hex}) contains the only imaginary frequency 1139.9*i* cm^{-1}, corresponding to the passage of the helium atom through the hexagon. In TS_{hex}, the helium atom lies in the plane of the 6-membered ring, and is equidistant from the carbon atoms ($L_{He\cdots C} = 1.578$ Å). The lengths of the 6.6 and 5.6 bonds of the penetrable hexagon are equal to 1.500 and 1.653 Å (in the pristine fullerene structure, they are 1.399 and 1.453 Å, respectively). The structure of TS_{hex} has a C_{3v} group point symmetry and the activation energy of this process is very high (939.7 kJ mol^{-1}).

The transition state of the alternative mode of helium penetration *via* the pentagon (TS_{pent}) has lower symmetry (C_s). Its carbon skeleton is more distorted compared to TS_{hex}, and the helium atom protrudes from the pentagon plane. The imaginary frequency and activation energy are 869.5*i* cm^{-1} and 1114.6 kJ mol^{-1}, respectively. Thus, the passage of the He atom through the hexagon is energetically more favorable because it has a lower activation barrier.

3.2 Formation of $He@C_{70}$ endofullerene. A correlation between the activation energies of helium penetration into fullerenes and squares of the hexagons

The C_{70} fullerene molecule has a D_{5h} symmetry point group, thus there are inequivalent atoms of 5 types $(a–e)^2$ and the number of possible modes of helium insertion increases. Taking into account the more favorable penetration through the hexagon obtained in the previous section, we have considered that the higher process

$$He + C_{70} \rightarrow He@C_{70} \quad (5)$$

probably occurs through the hexagons *abccba*, *ccdeed*, and *ddedde* (Fig. 4). Note that reaction (5) in contrast to the similar process (4) is slightly exothermic with the calculated heat effect of −5.4 kJ mol^{-1}. In the $He@C_{70}$ endofullerene, the helium atom lies at the center of the fullerene skeleton, which retains its initial D_{5h} symmetry. The PBE/3ζ-calculated structural

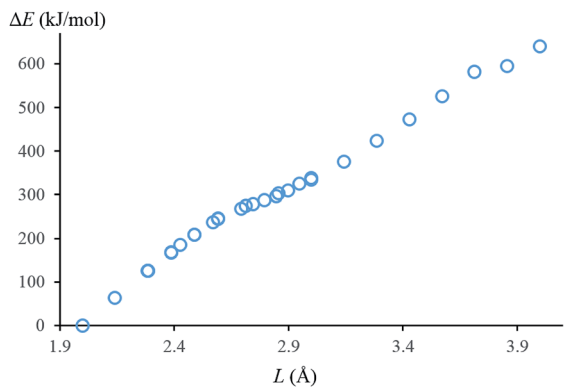

Fig. 1 Scanning of the triplet potential energy surface of the cleavage of the 5.6 bond of C_{60}. The DFT method used is PBE/3ζ. The range of the distances 2–3 Å were scanned more minutely because of the previously located energy minimum in this range.

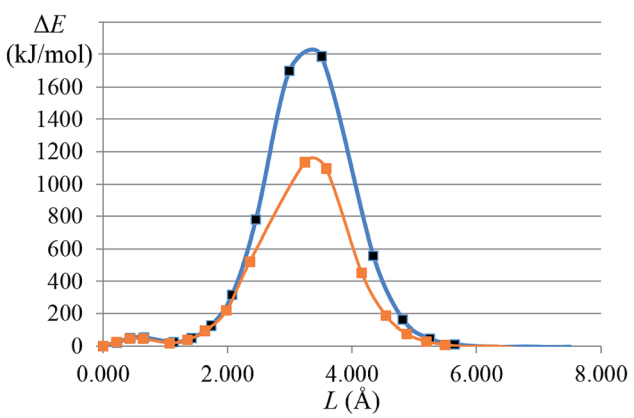

Fig. 2 Scanning of the singlet potential energy surfaces of helium penetration into the C_{60} fullerene *via* the pentagon (blue) and hexagon (orange) (the PBE/3ζ calculations).

Table 1 Structures of the transition states, imaginary frequencies, and activation energies of helium insertion into the C_{60} fullerene as calculated by the PBE/3ζ method

Transition state	L_{56}[a] (Å)	L_{66} (Å)	$L_{He\cdots C}$[b] (Å)	E_{act} (kJ mol^{-1})	ν_{imag} (cm^{-1})
$TS_{hex}(He + C_{60})$	1.653	1.5	1.578	939.7	1139.9*i*
$TS_{pent}(He + C_{60})$	1.533–2.248	—	1.571–1.591	1114.6	869.5*i*
$TS_{hex}(He + He@C_{60})$	1.654	1.5	1.578		1143.6*i*

[a] *L* is the carbon–carbon bond lengths in the penetrated polygon. [b] Hereinafter, the $L_{He\cdots C}$ values are the internuclear distances between the helium atoms and the carbon atoms of the polygons being penetrated.

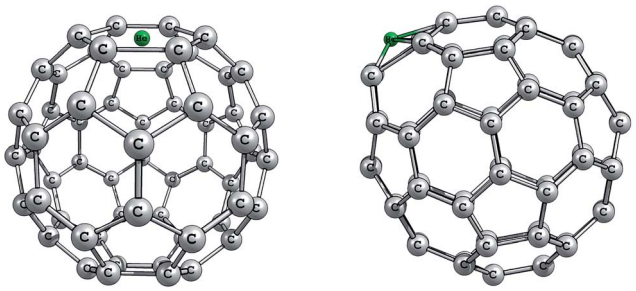

Fig. 3 Schematic of the transition states of helium penetration into the C_{60} fullerene through its hexagon (left) and pentagon (right).

parameters, imaginary frequencies, and activation energies are shown in Table 2. Their comparison indicates that helium more favorably penetrates through the hexagon *ccdeed* (the B3LYP/Λ1 calculations lead to qualitatively similar results; these values are given in the ESI Materials†).

We found a correlation between the activation energies of penetration and the squares of the hexagons penetrated (Fig. 5). As expected, the larger squares correspond to lower activation barriers. In the aspect of endofullerene chemistry, this correlation means that the activation barriers of the penetration into the fullerene cages do not vary significantly because the hexagons in the molecules of different fullerenes are characterized with almost the same bond lengths and therefore squares.

3.3 Formation of endofullerenes in terms of information entropy

Currently, the dihelium endofullerenes $He_2@C_{60}$ and $He_2@C_{70}$ have been synthesized, thus the ratios $[He@C_{60}] : [He_2@C_{60}]$ and $[He@C_{70}] : [He_2@C_{70}]$ measured are 200 : 1 and 20 : 1, respectively.[33,34] We calculated the activation energies of the second helium insertion into the C_{60} and C_{70} fullerene cages similarly to the first step. We found that the second processes are characterized with insignificantly higher activation energies (Tables 1 and 2; the calculated heat effects of formation of $He_2@C_{60}$ and $He_2@C_{70}$ from the respective mono-helium endofullerenes equal +44.5 and +18.5 kJ mol^{-1}). In the case of the C_{70} fullerene, the activation barriers of the second penetration mimic the first step and decrease in the series: *abccba* > *ddedde* > *ccdeed*. However, as follows from experimental studies,[33,34] the endofullerenes $He_2@C_{60/70}$ are formed in substantially lower amounts than their mono-encapsulated analogs. Therefore, the calculated energetic parameters cannot explain the experimentally observed regularities since the lowest activation energies of the first and second steps are related as ~1 : 1.

To solve this problem, we paid attention to the volumes of fullerene cages as different volume considerations (based on nuclear[65,66] and van der Waals volumes[65]) were previously used to explain the processes in fullerene-containing systems. We propose that the efficiency of the insertion process should correlate with the volume of the inner cavity. Therefore, when

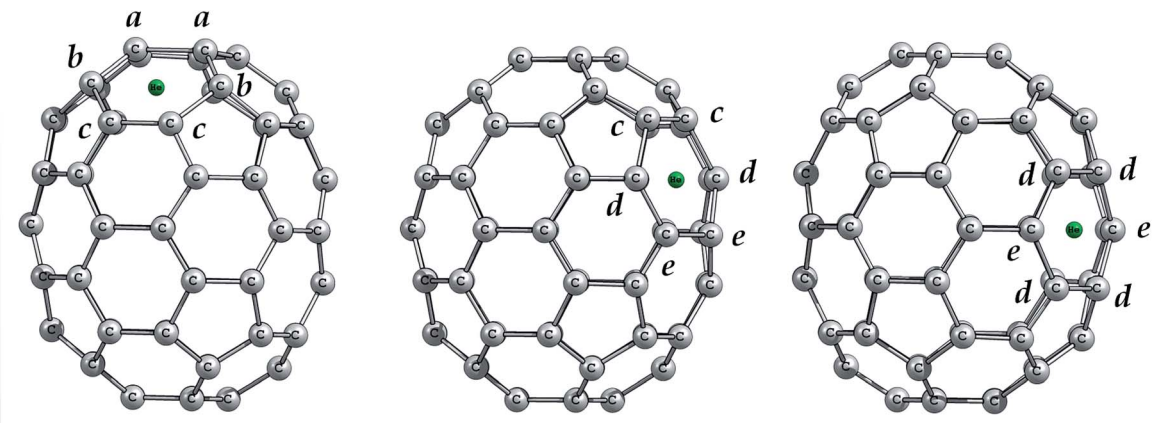

Fig. 4 Schematic of the transition states of helium penetration into the C_{70} fullerene through the hexagons *abccba* (left), *ccdeed* (center), and *ddedde* (right).

Table 2 Structures of the transition states, imaginary frequencies, and activation energies of helium insertion into the C_{70} fullerene as calculated by the PBE/3ζ method[a]

Transition state	L_{66}[b] (Å)	$L_{He\cdots C}$[b] (Å)	E_{act} (kJ mol^{-1})	ν_{imag} (cm^{-1})
TS_{abccba}(He + C_{70})	1.510 (*ab*), 1.629 (*bc*), 1.492 (*cc*), 1.658 (*aa*)	1.566–1.578	951.4	1164.0*i*
TS_{ccdeed}(He + C_{70})	1.487 (*cc*), 1.619 (*cd*), 1.539 (*de*), 1.677 (*ee*)	1.566–1.598	906.0	1122.0*i*
TS_{ddedde}(He + C_{70})	1.585 (*dd*), 1.558 (*de*)	1.553–1.587	936.8	1128.1*i*
TS_{abccba}(He + He@C_{70})	1.510 (*ab*), 1.630 (*bc*), 1.492 (*cc*), 1.658 (*aa*)	1.566–1.580	955.3	1165.0*i*
TS_{ccdeed}(He + He@C_{70})	1.487 (*cc*), 1.619 (*cd*), 1.539 (*de*), 1.679 (*ee*)	1.567–1.598	911.1	1124.1*i*
TS_{ddedde}(He + He@C_{70})	1.585 (*dd*), 1.558 (*de*)	1.553–1.587	941.3	1130.9*i*

[a] The designations of the bond are shown in Fig. 4. [b] See the footnotes to Table 1.

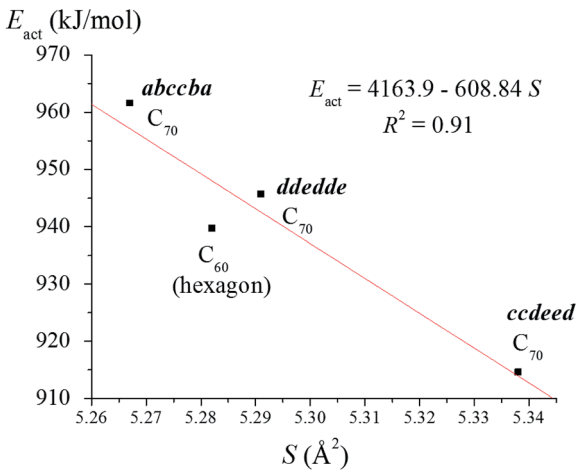

Fig. 5 Linear correlation between the activation energies of helium penetration into C_{60} and C_{70} through the hexagons and their squares *S*.

the first helium atom gets inside, the inner cavity volume becomes smaller, and consequently, the yields of the dihelium endofullerenes are decreased. The abovementioned numerical results corresponding to the considerations are shown in Table 3. In the table, indices 1 and 2 designate the first and the second steps of insertion. The V_1 values are the values of the inner cavities of C_{60} and C_{70} taken from the study of Adams *et al.*[65] and $V_2 = V_1 - V_{He}$ (V_{He} is the van der Waals volume of helium deduced from ref. 67). Unfortunately, the $V_1 : V_2$ ratios are quite close for different fullerenes; therefore, the inner cavity volumes do not reproduce the experimental ratios [He@C_{60}] : [He_2@C_{60}] and [He@C_{70}] : [He_2@C_{70}].

Previously, the proposition has been made that the stochastic processes (which are not defined by the energetic factor) in fullerene-containing systems may be described in terms of information entropy.[62,63] This is a structural index that shows the diversity of the molecular system deduced from the number of inequivalent atoms.[56,57] Within such approach, the molecule is considered a message and its atoms symbols. The atoms of one element located in the same positions belong to one type. This index increases with the number of different atom types in the molecules and its lower molecular structure values are associated with the higher likelihood of their formation in non-equilibrium conditions.[68] Indeed, the use of this quantity allows us to discriminate 14 experimentally achievable fullerenes (including C_{60} and C_{70}) from 2079 possible fullerene structures.[62] Later, the information-entropy approach was extrapolated to oxygen allotropes.[63] This encouraged us to analyze the complexity of the title endofullerenes and their analogs with other fillings. For this purpose, we considered together the endofullerenes produced with "hard" (pressure induced) and "gentle" (molecular surgery[69]) synthetic methodologies. Although these approaches essentially differ in their implementations, the underlying processes of insertion have a probabilistic nature.

The calculated information entropies of the endofullerenes are shown in Table 4. We include in our study the cases for which the ratios of singly and doubly encapsulated fullerenes were measured. These are, in addition to helium endofullerenes, their analogs with encapsulated neon atoms,[70] He⋯N species,[64] hydrogen,[71] and water[72] molecules. The geometries of these endofullerenes were taken from previous studies to calculate the information entropies according to eqn (3).

We calculated the changes in information entropy Δh upon the encapsulation according to Karreman's work[73] considering that this value is similar to the other thermodynamic functions of physical and chemical processes as the difference between the initial and final values:

$$\Delta h = \sum_{\text{products}} h_i - \sum_{\text{reactants}} h_j \qquad (6)$$

As previously shown,[62,68] the lower information entropies correspond to a higher probability of chemical structure. In our

Table 3 Ratios of the activation and volume parameters of the subsequent processes resulting in singly and doubly filled endofullerenes

Process	V_1 (Å^3)	V_2 (Å^3)	$V_1 : V_2$	E_{act1} (kJ mol^{-1})	E_{act2} (kJ mol^{-1})	$E_{act1} : E_{act2}$
nHe + C_{60} → He_n@C_{60}	34.5	23.0	1.5 : 1	936.6	934.8	~1 : 1
nHe + C_{70} → He_n@C_{70}	51.1	39.6	1.3 : 1	906.0	911.1	~1 : 1

Table 4 Symmetries, partitions, and information entropies of C_{60}, C_{70}, and their endohedral complexes

Molecule[a]	Symmetry	Partition	h (bits)
C_{60}	I_h	1×60	0.000
He@C_{60}	I_h	$1 \times 60 + 1 \times 1$	0.121
He_2@C_{60}	D_{5d}	$2 \times 20 + 2 \times 10 + 1 \times 2$	2.062
HeN@C_{60}	C_{3v}	$9 \times 6 + 2 \times 3 + 2 \times 1$	3.549
C_{70}	D_{5h}	$2 \times 20 + 3 \times 10$	2.236
He@C_{70}	D_{5h}	$2 \times 20 + 3 \times 10 + 1 \times 1$	2.311
He_2@C_{70}	D_{5h}	$2 \times 20 + 3 \times 10 + 1 \times 2$	2.357
Ne_2@C_{70}	D_{5h}	$2 \times 20 + 3 \times 10 + 1 \times 2$	2.357
HeN@C_{70}	C_{5v}	$5 \times 10 + 4 \times 5 + 2 \times 1$	3.218
H_2@C_{70}	D_{5h}	$2 \times 20 + 3 \times 10 + 1 \times 2$	2.357
$(H_2)_2$@C_{70}	C_1	74×1	6.209
H_2O@C_{70}	C_1	73×1	6.190
$(H_2O)_2$@C_{70}	C_1	76×1	6.248

[a] Small homoatomic species have zero h values; $h = 1$ and 0.918 in the case of He···N and H_2O, respectively (according to eqn (3)).

cases, all the calculated Δh values are positive, which reflects the lower probability of the encapsulated fullerenes as compared to the empty fullerenes. A lower Δh should correspond to higher yields of the endofullerenes:

$$\Delta h \sim \frac{1}{[\text{product}]} \tag{7}$$

or applied to our case:

$$\Delta h_1 \sim \frac{1}{[\text{X@C}_{60/70}]} \text{ and } \Delta h_{\text{tot}} \sim \frac{1}{[\text{2X@C}_{60/70}]} \tag{8}$$

where $\Delta h_{\text{tot}} = \Delta h_1 + \Delta h_2$ and indices 1 and 2 correspond to the first and the second steps of insertion. Therefore, the following ratio should relate to the observed yields of endofullerenes:

$$[\text{X@C}_{60/70}] : [\text{2X@C}_{60/70}] \sim \Delta h_{\text{tot}} : \Delta h_1 \tag{9}$$

The results of the calculations are presented in Table 5. As observed from the table, the ratios $\Delta h_{\text{tot}} : \Delta h_1$ and $[\text{X@C}_{60/70}] : [\text{2X@C}_{60/70}]$ do not precisely match. However, we may note that there is a qualitative relation between the calculated and experimental values. For example, the relation of the $\Delta h_{\text{tot}} : \Delta h_1$ values indicates a 10.6 times higher possibility of dihelium endofullerene formation in the case of C_{70} as compared to C_{60} (this estimate is calculated by the division of the respective $\Delta h_{\text{tot}} : \Delta h_1$ values). The value deduced from the experimental ratio of $[\text{X@C}_{70}] : [\text{2X@C}_{70}]/[\text{X@C}_{60}] : [\text{2X@C}_{60}]$ equals to 10. We additionally included in Table 5 helium–nitrogen endofullerenes although the ratios of the singly and doubly encapsulated species after formation are unknown. Nevertheless, ref. 64 demonstrated the lower probability of formation of HeN@C_{60} than HeN@C_{70} as compared with their singly filled precursors. Such ratio follows from the calculated $\Delta h_{\text{tot}} : \Delta h_1$ values (29 : 1 *vs.* 13 : 1).

Of course, we should note the disadvantages of the information entropy approach. It implies that isostructural endofullerenes (having the same symmetry but differing in the type of encapsulated atoms) demonstrate the same h and $\Delta h_{\text{tot}} : \Delta h_1$ values, and according to the approach, the same experimental ratios of singly and doubly filled endofullerenes. This does not take into account the size of the guest. The size should not be neglected: for example, the experiments suggest that the probability of He_2@C_{70} formation is higher than Ne_2@C_{70},[33,70] which is a consequence of the larger volume of the neon atom.

Another case, which is not described within our approach, is water molecules inside the C_{70} fullerene. The information entropy calculations predict the almost equiprobable formation of H_2O@C_{70} and $(H_2O)_2$@C_{70} (or even somewhat more probable formation of the doubly filled compound with the ratio 1 : 1.4). This, unfortunately, contradicts the experimental results of ref. 72, in which the water dimer inside the C_{70} cage is synthesized in substantially smaller amounts. We will analyze the reasons for this mismatch in further studies.

Despite the mentioned disadvantage and qualitative nature of the obtained relations, the information entropy approach demonstrates agreement with the experimental data better than the other approaches based on activation parameters and volume considerations.

4 Conclusions

In the present study, we calculated the activation barriers of helium penetration into the C_{60} and C_{70} fullerenes resulting in

Table 5 Information entropies of the first and the second insertions into the fullerenes, their ratios, and experimental ratios of the singly and doubly filled endofullerenes

Processes	Δh_1	Δh_2	Δh_{tot}	$\Delta h_{\text{tot}} : \Delta h_1$	$[\text{X@C}_{60/70}] : [\text{2X@C}_{60/70}]$ (reference)
nHe + C_{60} → He_n@C_{60}	0.121	1.941	2.062	17 : 1	200 : 1 (ref. 34)
nHe + C_{70} → He_n@C_{70}	0.075	0.046	0.121	1.6 : 1	20 : 1 (ref. 33)
nNe + C_{70} → Ne_n@C_{70}	0.075	0.046	0.121	1.6 : 1	50 : 1 (ref. 70)
$n$$H_2$ + C_{70} → $(H_2)_n$@C_{70}	0.121	3.852	3.973	33 : 1	32 : 1 (ref. 71)
He + N + C_{60} → HeN@C_{60}	0.121[a]	3.428[b]	3.549	29 : 1	—
He + N + C_{70} → HeN@C_{70}	0.075[a]	0.907[b]	0.982	13 : 1	~3 : 1 (ref. 64)[c]
$n$$H_2O$ + C_{70} → $(H_2O)_n$@C_{70}	3.036	−0.86	2.176	1 : 1.4	—

[a] For the process: He + $C_{60/70}$ → He@$C_{60/70}$. [b] For the process: N + He@$C_{60/70}$ → NHe@$C_{60/70}$. [c] The value $[\text{He@C}_{70}] : [\text{HeN@C}_{70}]$ is obtained from the mass spectra of the products after purification and therefore it does not reflect the ratio of the products after formation, but notwithstanding shows that the doubly encapsulated endofullerene is formed in smaller amounts.

singly and doubly filled endofullerenes. For the example of C_{60}, we demonstrated the higher favorability of the hexagon than pentagon to be penetrated. The barriers of hexagon penetration of C_{60} and C_{70} are comparably high ($\sim$900 kJ mol^{-1}) and do not significantly differ for the two subsequent steps of insertion. Their correlation with the square of the penetrated hexagons has been found. This correlation allows the proposal that the other fullerene cages should reveal almost the same penetrability since the size of the hexagons do not significantly vary from one fullerene to another.

We have shown that the experimental ratios of the yields of X@$C_{60/70}$ and 2X@$C_{60/70}$ are qualitatively described in terms of the information entropy approach using the respective changes in information entropy upon the formation of singly and doubly filled fullerenes. Despite some disadvantages, this approach takes into account the probabilistic nature of the penetration processes. We think that the information approach may be used in future for better understanding of the processes underlying endofullerene formation.

Acknowledgements

The authors are grateful to Russian Foundation for Basic Research (Russia) for financial support (projects 14-03-00467 and 16-03-00822).

Notes and references

1 D. S. Bethune, R. D. Johnson, J. R. Salem, M. S. de Vries and C. S. Yannoni, *Nature*, 1993, **366**, 123.
2 V. I. Sokolov, *Russ. Chem. Bull.*, 1993, **42**, 1.
3 S. Liu and S. Sun, *J. Organomet. Chem.*, 2000, **599**, 74.
4 S. Guha and K. Nakamoto, *Coord. Chem. Rev.*, 2005, **249**, 1111.
5 V. I. Sokolov and I. V. Stankevich, *Russ. Chem. Rev.*, 1993, **62**, 419.
6 A. A. Popov, S. Yang and L. Dunsch, *Chem. Rev.*, 2013, **113**, 5989.
7 S. Osuna, M. Swart and M. Solà, *Chem.–Eur. J.*, 2009, **15**, 13111.
8 T. Weiske, D. K. Boehme and H. Schwarz, *J. Phys. Chem.*, 1991, **95**, 8451.
9 T. Weiske, T. Wong, W. Krätschmer, J. K. Terlouw and H. Schwarz, *Angew. Chem., Int. Ed. Engl.*, 1992, **31**, 183–185.
10 R. Kleiser, H. Sprang, S. Furrer and E. E. B. Campbell, *Z. Phys. D: At., Mol. Clusters*, 1993, **28**, 89.
11 M. Saunders, H. A. Jiménez-Vázquez, R. J. Cross, S. Mroczkowski, D. I. Freedberg and F. A. L. Anet, *Nature*, 1994, **367**, 256.
12 M. Saunders, R. J. Cross, H. A. Jimenez-Vazquez, R. Shimshi and A. Khong, *Science*, 1996, **271**, 1693.
13 M. Saunders, H. A. Jimenez-Vazquez, R. J. Cross and R. J. Poreda, *Science*, 1993, **259**, 1428.
14 J. J. L. Morton, A. M. Tyryshkin, A. Ardavan, S. C. Benjamin, K. Porfyrakis, S. A. Lyon and G. A. D. Briggs, *Phys. Status Solidi B*, 2006, **243**, 3028.
15 S. C. Benjamin, A. Ardavan, G. A. D. Briggs, D. A. Britz, D. Gunlycke, J. Jefferson, M. A. G. Jones, D. F. Leigh, B. W. Lovett, A. N. Khlobystov, S. A. Lyon, J. J. L. Morton, K. Porfyrakis, M. R. Sambrook and A. M. Tyryshkin, *J. Phys.: Condens. Matter*, 2006, **18**, S867.
16 S. Schaefer, K. Huebener, W. Harneit, C. Boehme, K. Fostiropoulos, H. Angermann, J. Rappich, J. Behrends and K. Lips, *Solid State Sci.*, 2008, **10**, 1314.
17 K. Akiyama, H. Haba, K. Tsukada, M. Asai, A. Toyoshima, K. Sueki, Y. Nagame and M. Katada, *J. Radioanal. Nucl. Chem.*, 2009, **280**, 329.
18 J. Cioslowski and E. D. Fleischmann, *J. Chem. Phys.*, 1991, **94**, 3730.
19 W. Even, J. Smith and M. W. Roth, *Mol. Simul.*, 2005, **31**, 207.
20 A. A. Levin and N. N. Breslavskaya, *Russ. Chem. Bull.*, 2005, **54**, 1999.
21 S. Osuna, M. Swart and M. Solà, *Phys. Chem. Chem. Phys.*, 2011, **13**, 3585.
22 Z.-Y. Wang, K.-H. Su, X.-P. Yao, Y.-L. Li and F. Wang, *Mater. Chem. Phys.*, 2010, **119**, 406.
23 H. Yan, S. Yu, X. Wang, Y. He, W. Huang and M. Yang, *Chem. Phys. Lett.*, 2008, **456**, 223.
24 D. S. Sabirov and R. G. Bulgakov, *JETP Lett.*, 2010, **92**, 662.
25 A. V. Marenich, C. J. Cramer and D. G. Truhlar, *Chem. Sci.*, 2013, **4**, 2349.
26 J. A. Ludlow, T.-G. Lee and M. S. Pindzola, *J. Phys. B: At., Mol. Opt. Phys.*, 2010, **43**, 235202.
27 R. L. Murry and G. E. Scuseria, *Science*, 1994, **263**, 791–793.
28 S. Patchkovskii and W. Thiel, *J. Am. Chem. Soc.*, 1996, **118**, 7164.
29 S. Patchkovskii and W. Thiel, *J. Am. Chem. Soc.*, 1998, **120**, 556.
30 J. Hrušák, D. K. Böhme, T. Weiske and H. Schwarz, *Chem. Phys. Lett.*, 1992, **193**, 97.
31 E. Ōsawa, *Fullerenes, Nanotubes, Carbon Nanostruct.*, 2012, **20**, 299.
32 D. Heymann, S. M. Bachilo and S. Aronson, *Fullerenes, Nanotubes, Carbon Nanostruct.*, 2005, **13**, 73.
33 A. Khong, H. A. Jiménez-Vázquez, M. Saunders, R. J. Cross, J. Laskin, T. Peres, C. Lifshitz, R. Strongin and A. B. Smith, *J. Am. Chem. Soc.*, 1998, **120**, 6380.
34 T. Sternfeld, R. E. Hoffman, M. Saunders, R. J. Cross, M. S. Syamala and M. Rabinovitz, *J. Am. Chem. Soc.*, 2002, **124**, 8786.
35 D. S. Sabirov, *J. Phys. Chem. C*, 2013, **117**, 1178.
36 D. S. Sabirov, A. A. Tukhbatullina and R. G. Bulgakov, *Fullerenes, Nanotubes, Carbon Nanostruct.*, 2015, **23**, 835.
37 D. S. Sabirov, A. O. Terentyev, I. S. Shepelevich and R. G. Bulgakov, *Comput. Theor. Chem.*, 2014, **1045**, 86.
38 J. P. Perdew, K. Burke and M. Ernzerhof, *Phys. Rev. Lett.*, 1996, **77**, 3865.
39 D. N. Laikov and Y. A. Ustynyuk, *Russ. Chem. Bull.*, 2005, **54**, 820.
40 D. S. Sabirov, R. G. Bulgakov and S. L. Khursan, *ARKIVOC*, 2011, **8**, 200.
41 D. S. Sabirov, *RSC Adv.*, 2014, **4**, 44996.
42 A. F. Shestakov, *Russ. J. Gen. Chem.*, 2008, **78**, 811.

43 D. S. Sabirov, R. G. Bulgakov, S. L. Khursan and U. M. Dzhemilev, *Dokl. Phys. Chem.*, 2009, **425**, 54.
44 A. R. Tuktarov, A. R. Akhmetov, D. S. Sabirov, L. M. Khalilov, A. G. Ibragimov and U. M. Dzhemilev, *Russ. Chem. Bull.*, 2009, **58**, 1724.
45 D. S. Sabirov and R. G. Bulgakov, *Fullerenes, Nanotubes, Carbon Nanostruct.*, 2010, **18**, 455.
46 A. R. Tuktarov, V. V. Korolev, D. S. Sabirov and U. M. Dzhemilev, *Russ. J. Org. Chem.*, 2011, **47**, 41.
47 D. S. Sabirov, R. R. Garipova and R. G. Bulgakov, *J. Phys. Chem. A*, 2013, **117**, 13176.
48 D. S. Sabirov, S. L. Khursan and R. G. Bulgakov, *Fullerenes, Nanotubes, Carbon Nanostruct.*, 2008, **16**, 534.
49 D. S. Sabirov, R. R. Garipova and R. G. Bulgakov, *Fullerenes, Nanotubes, Carbon Nanostruct.*, 2015, **23**, 1051.
50 D. R. Diniakhmetova, A. K. Friesen and S. V. Kolesov, *Int. J. Quantum Chem.*, 2016, **116**, 489.
51 A. D. Becke, *J. Chem. Phys.*, 1993, **98**, 5648.
52 D. N. Laikov, *Chem. Phys. Lett.*, 2005, **416**, 116.
53 Z. Y. Wang, K. H. Su, H. Q. Fan, Y. L. Li and Z. Y. Wen, *Mol. Phys.*, 2008, **106**, 703.
54 D. S. Sabirov, *J. Phys. Chem. C*, 2013, **117**, 9148.
55 D. Bonchev, D. Kamenski and V. Kamenska, *Bull. Math. Biol.*, 1976, **38**, 119.
56 D. Bonchev and N. Trinajstić, *J. Chem. Phys.*, 1977, **67**, 4517.
57 Y. A. Zhdanov, *Information Entropy in Organic Chemistry*, Rostov University, 1979.
58 D. Bonchev, O. V. Mekenyan and N. Trinajstić, *J. Comput. Chem.*, 1981, **2**, 127.
59 D. K. Agrafiotis, *J. Chem. Inf. Model.*, 1997, **37**, 576–580.
60 J. W. Godden, F. L. Stahura and J. Bajorath, *J. Chem. Inf. Model.*, 2000, **40**, 796.
61 S. J. Barigye, Y. Marrero-Ponce, F. Pérez-Giménez and D. Bonchev, *Mol. Diversity*, 2014, **18**, 673.
62 D. S. Sabirov and E. Ōsawa, *J. Chem. Inf. Model.*, 2015, **55**, 1576.
63 D. S. Sabirov and I. S. Shepelevich, *Comput. Theor. Chem.*, 2015, **1073**, 61.
64 Y. Morinaka, S. Sato, A. Wakamiya, H. Nikawa, N. Mizorogi, F. Tanabe, M. Murata, K. Komatsu, K. Furukawa, T. Kato, S. Nagase, T. Akasaka and Y. Murata, *Nat. Commun.*, 2013, **4**, 1554.
65 G. B. Adams, M. O'Keeffe and R. S. Ruoff, *J. Phys. Chem.*, 1994, **98**, 9465.
66 D. S. Sabirov, A. D. Zakirova, A. A. Tukhbatullina, I. M. Gubaydullin and R. G. Bulgakov, *RSC Adv.*, 2013, **3**, 1818.
67 J. Emsley, *The Elements*, Clarendon Press; Oxford University Press, Oxford, New York, 3rd edn, 1998.
68 V. M. Talanov and V. V. Ivanov, *Russ. J. Gen. Chem.*, 2013, **83**, 2225.
69 M. Murata, Y. Murata and K. Komatsu, *Chem. Commun.*, 2008, 6083.
70 J. Laskin, T. Peres, C. Lifshitz, M. Saunders, R. J. Cross and A. Khong, *Chem. Phys. Lett.*, 1998, **285**, 7.
71 M. Murata, S. Maeda, Y. Morinaka, Y. Murata and K. Komatsu, *J. Am. Chem. Soc.*, 2008, **130**, 15800.
72 R. Zhang, M. Murata, T. Aharen, A. Wakamiya, T. Shimoaka, T. Hasegawa and Y. Murata, *Nat. Chem.*, 2016, **8**, 435.
73 G. Karreman, *Bull. Math. Biophys.*, 1955, **17**, 279.